

CO Adsorbed Infrared Spectroscopy Study of Ni/Al₂O₃ Catalyst for CO₂ Reforming of Methane

Xinli Zhu · Yue-ping Zhang · Chang-jun Liu

Received: 29 May 2007 / Accepted: 5 July 2007 / Published online: 25 July 2007
© Springer Science+Business Media, LLC 2007

Abstract CO adsorbed infrared spectroscopy study was conducted in this work in order to better understand the significantly improved anti-coke performance of Ni/Al₂O₃ catalyst obtained via argon glow discharge plasma treatment. The present study revealed a significant decrease of linear to bridge (L/B) adsorbed CO for glow discharge plasma treated Ni/Al₂O₃, compared to that for untreated Ni/Al₂O₃, indicating an enhancement of close packed plane concentration. This structure change leads to lower methane turnover frequency (TOF) and better balance of carbon formation-gasification, resulting in better anti-coke property of Ni/Al₂O₃ for CO₂ reforming of methane.

Keywords Methane · CO₂ reforming · Ni/Al₂O₃ · CO adsorbed infrared spectroscopy · Plasma · Coke

1 Introduction

Carbon dioxide reforming of methane to synthesis gas (CO and H₂) attracts ever-growing interest from both environmental and industry aspects [1, 2]. Deactivation of Ni-based catalyst due to coke formation is a big obstacle for industry application. Therefore, control of coke formation is of great importance for both fundamental study and application.

The morphology of Ni particles has significant effect on the long-term stability of the catalyst. It is generally accepted that methane dissociation over Ni is the rate-determining step of CO₂ reforming of methane [3, 4]. Methane dissociation is structure sensitive, with higher activation energy over close packed planes (high coordinated sites, such as Ni(111)) than that over defect sites or open planes (low coordinated sites, such as Ni(100)) [5–7]. Therefore, methane dissociation over defect sites are faster, giving rise to large amount of monatomic of carbon over these defect sites during CO₂ reforming. If such formed carbon cannot be immediately gasified by CO₂, they will nucleate and polymerize over the surface of Ni particle to form encapsulating carbon or diffuse through the Ni particle and precipitate at the Ni-support interface to form filamentous carbon [8]. Both encapsulating carbon and filamentous carbon are harmful for catalytic run [8].

A general approach to elimination of coke formation is to selective block part of defect sites using inert element atoms [9–11], such as S, Sn, K and so on. For example, Nielsen et al. reported sulfur passivated Ni catalyst showed long-term stability for CO₂ reforming [9]. This approach is usually accompanied by an activity decrease.

CO adsorption combined with infrared spectroscopy (IR) is extensively used to probe the structure of supported transition metal catalysts, especially for the CO involved

X. Zhu · C.-j. Liu (✉)
Key Laboratory for Green Chemical Technology of Ministry of Education, School of Chemical Engineering, Tianjin University, Tianjin 300072, China
e-mail: ughg_cjl@yahoo.com

X. Zhu
e-mail: xinlizhu@ou.edu

Y.-p. Zhang
Department of Chemistry, Tianjin University, Tianjin 30072, China

Present Address:
X. Zhu
School of Chemical, Biological and Materials Engineering,
The University of Oklahoma, Norman, OK 73019, US
e-mail: xinlizhu@ou.edu

reaction, such as CO hydrogenation and reforming reactions.

In this work, we use CO adsorbed IR to probe the surface structure, i.e., morphology, of argon glow discharge plasma treated Ni/Al₂O₃ catalyst, and correlate the structure changes with anti-coke property of CO₂ reforming of methane.

2 Experimental

The two Ni/Al₂O₃ ($W_{\text{Ni}}:W_{\text{alumina}} = 5:100$) catalysts were prepared by incipient wetness impregnations with and without plasma treatment. The γ -Al₂O₃ powder (provided by Institute of Chemical Engineering, Tianjin. $S_{\text{BET}} = 230 \text{ m}^2/\text{g}$) was calcined at 600 °C for 4 h prior to use. It was impregnated with an aqueous solution of Ni(NO₃)₂ at room temperature for 12 h, and dried at 110 °C for 12 h. After that, the sample was treated with plasma. The obtained sample was then calcined at 600 °C for 4 h. It was referred to as NiAl-PC. A comparison sample without plasma treatment was denoted as NiAl-C.

The plasma treatment was carried out at room temperature in a glow discharge system [12], as shown in Fig. 1. Catalyst powder (about 0.5 g), loaded in a quartz boat, was put into the discharge cell. After the pressure was adjusted in the range of 100 to 200 Pa, the discharge was initiated by applying voltage of 900 V to the electrodes using a high voltage amplifier (Trek, 20/20B). The signal input for the high voltage amplifier was supplied by a function/arbitrary waveform generator (Hewlett Packard, 33120A) with a 100 Hz square wave. Ultrahigh pure grade argon (>99.999%) was used as the plasma-forming gas. During the plasma treatment, the surface of the sample turned from green to dark brown. The time of each plasma treatment was 10 min and each sample was treated 5 times.

Catalytic performance was carried out in a quartz tube with an inner diameter of 4 mm at ambient pressure. A

catalyst sample of 50 mg (40–60 mesh) was packed in the quartz tube with two layers of quartz wool. It was reduced in situ by flowing H₂ at 700 °C for 2 h. The feed gases of CH₄ and CO₂ diluted in Ar (the ratio of CH₄:CO₂:Ar is 1:1:2) were introduced into the micro reactor by mass flow controllers at 750 °C. The gas hourly space velocity (GHSV) was $4.8 \times 10^4 \text{ cm}^3/(\text{g-cat}\cdot\text{h})$. The gases were ultra high pure grade (>99.999%) and were used without further purification. The gas residue was analyzed online by a gas chromatograph (Agilent 6890). The reaction time was 5 h. After reaction, the catalyst was cooled to 40 °C under flowing argon. An in situ temperature programmed oxidation (TPO) was then carried out using 3% O₂/He flow to evaluate the coke formed over the catalysts. The ramp rate was 10 °C/min. The products of CO₂ ($m/z = 44$) and CO ($m/z = 28$) were monitored by a mass spectrometer (GSD301, OmmistarTM).

Diffuse reflectance Fourier transform infrared spectra were recorded on a Tensor 27 spectrometer (Bruker) equipped with a liquid nitrogen cooled Mercury-Cadmium-Tellurium (MCT) detector, a diffuse reflectance accessory (Praying Mantis, Harrick), and a high temperature reaction chamber (HVC, Harrick). The high temperature cell was fitted with two CaF₂ windows. The catalyst sample was firstly reduced ex situ at 700 °C for 2 h using flowing H₂. The resulted catalyst powder (approximately 35 mg) was loaded in the sample cup of the high temperature cell. It was then reduced in situ at 300 °C for 1 h using flowing H₂ and then flushed with a flow of He for 30 min. The sample was then cooled to 25 °C. At this time, a background spectrum was recorded. 1.1 kPa of CO in He flowed through the sample cup at 25 °C for 30 min. Then the cell was purged with flowing He for another 30 min. After that the temperature was increased to 400 °C at a rate of 10 °C/min. The IR spectra were recorded at a resolution of 4 cm⁻¹ and 64 scans with background spectrum subtracted. All spectra were presented in Kubelka-Munk units, since its intensity is linear with the surface species concentration. Transmission electron microscopy (TEM) observations were performed on a Philips TECNAI G²F20 system to evaluate the Ni particle size of fresh reduced Ni/Al₂O₃ catalysts. X-ray powder diffraction (XRD) patterns were recorded by a Rigaku D/max-2500 diffractometer with Cu K α radiation source ($\lambda = 1.54056 \text{ \AA}$).

3 Results and Discussions

3.1 IR Study of CO Adsorption

The IR spectra of CO adsorbed on NiAl-C and NiAl-PC at 25 °C are shown in Fig. 2A and 2B, respectively. When 1.1 kPa CO was introduced for 1 min, a band at 1933 cm⁻¹

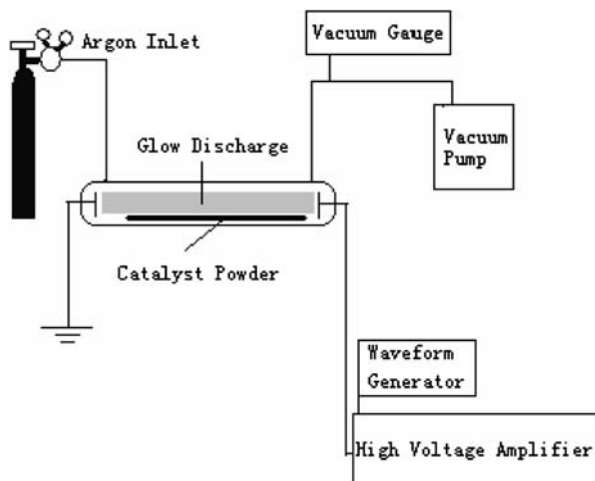
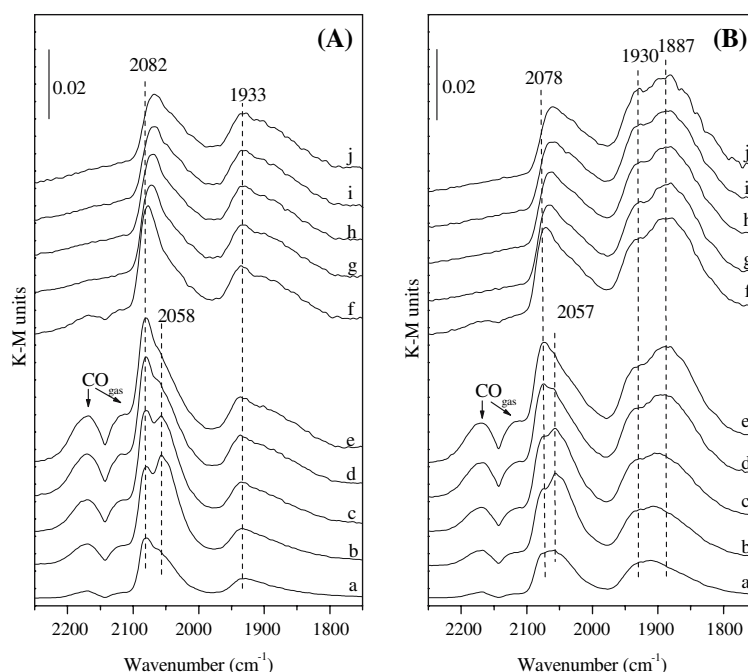


Fig. 1 Schematic representation of plasma treatment setup

Fig. 2 IR spectra of CO adsorbed on reduced (A) NiAl-C and (B) NiAl-PC samples. The samples were exposed to 1.1 kPa CO for (a) 1 min; (b) 5 min; (c) 10 min; (d) 20 min; (e) 30 min; and purged with He for (f) 1 min; (g) 5 min; (h) 10 min; (i) 20 min; (j) 30 min



and a band at 2082 cm^{-1} , with a shoulder at 2058 cm^{-1} , were developed for the NiAl-C sample (a). As the exposure time increased to 5 min, the intensities of all bands increased. The shoulder band at 2058 cm^{-1} became more intense than the 2082 cm^{-1} band (b). At 10 min, the bands at 2058 cm^{-1} and at 2082 cm^{-1} had similar intensities (c). At 20 min, the band at 2082 cm^{-1} became the predominant band (d). As exposure time was further increased, the bands did not change their intensities (e), indicating that the CO adsorption equilibrium was obtained at $25\text{ }^{\circ}\text{C}$. A CO desorption was then performed at $25\text{ }^{\circ}\text{C}$ (f, g, h, i, j). The band at 2082 cm^{-1} lost its intensity and the peak shifted to 2068 cm^{-1} after 30 min of desorption. In contrast, the lower frequency band at 1933 cm^{-1} remained unchanged. A similar IR band evolution process was observed for the sample of NiAl-PC during exposure to CO and desorption, as shown in Fig. 2B.

However, the band locations and intensities are different for the two samples. The equilibrium intensities of the gaseous phase CO bands are identical for the two samples, which means it is reasonable to compare both the band locations and intensities. For the NiAl-PC sample, the higher frequency band and its shoulder shift to 2078 cm^{-1} and 2057 cm^{-1} , respectively. The lower frequency band is at 1930 cm^{-1} , and a new band centered at 1887 cm^{-1} is present, which cannot be observed in the NiAl-C.

For the purpose of comparison, the IR spectra of NiAl-C and NiAl-PC after desorption at $25\text{ }^{\circ}\text{C}$ for 30 min (Fig. 2j) are shown in Fig. 3. The spectra of CO desorption at $150\text{ }^{\circ}\text{C}$ are also illustrated in Fig. 3. When the temperature was increased to $150\text{ }^{\circ}\text{C}$, the high frequency band significantly lost its intensity and down shifted to 2021 cm^{-1} and

2010 cm^{-1} for NiAl-C and NiAl-PC, respectively. For NiAl-C, the low frequency band shifted to 1910 cm^{-1} , and its intensity slightly increased. This result suggests that the high frequency band changes to the low frequency band when the temperature is increased. For NiAl-PC, the band at 1930 cm^{-1} is no longer present, and a band at 1883 cm^{-1} appears. The band at 1883 cm^{-1} is most probably a consequence of the band at 1930 cm^{-1} shifting to lower wavenumbers and merging with the band at 1881 cm^{-1} .

Generally, the high frequency band at $2100\text{--}2000\text{ cm}^{-1}$ can be assigned to linear adsorbed CO on Ni^0 , and the low frequency band at $2000\text{--}1750\text{ cm}^{-1}$ is attributed to two or three fold bridge adsorbed CO on Ni^0 [13–25]. The band at 2058 cm^{-1} is initially more intense than the band at 2082 cm^{-1} . But as the exposure time (CO coverage) increases, the band at 2082 cm^{-1} prevails. Moreover, the band at 2082 cm^{-1} is more easily removed during the desorption process, indicating that it is weakly adsorbed CO. Thus we assign the band at 2058 cm^{-1} to one CO molecule linearly bonded to one Ni atom, and the band at 2082 cm^{-1} to two or three CO molecules bonded to one Ni atom (subcarbonyl species). This assignment is in agreement with Rochester and Terrell [18], who ascribed the band at $2065\text{--}2090\text{ cm}^{-1}$ to subcarbonyl species, and the band at $2030\text{--}2050\text{ cm}^{-1}$ to isolated linear CO. Their assignments were lately confirmed by Blackmond and Ko [19]. We assign the band at 1930 cm^{-1} and 1887 cm^{-1} to one CO molecule bridge bonded to two Ni atoms and to three Ni atoms, respectively.

The $\text{Ni}(\text{CO})_4$ species (nickel carbonyl species) is not observed in the present study, which is favorably formed at low temperature and high CO pressure [26, 27], and its sharp and strong IR band is located at ca. 2047 cm^{-1}

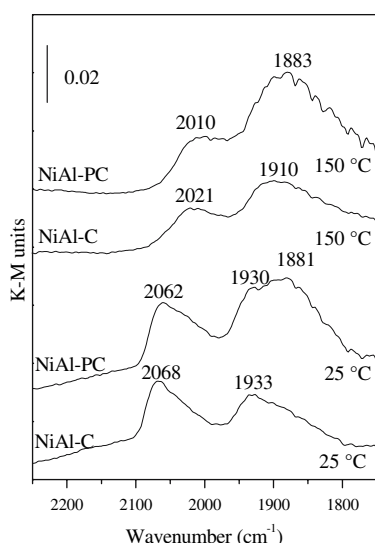


Fig. 3 Comparison of IR spectra of CO desorption for NiAl-C and NiAl-PC at 25 °C and 150 °C

[22–24]. In a recent study of Derrouiche and Bianchi [25], they studied the IR spectra of 1% CO/He adsorption on 20% Ni/Al₂O₃, which is similar to our conditions. Also, no Ni(CO)₄ species was observed [25].

The ratio of integrated intensities of linearly adsorbed CO to bridge adsorbed CO (L/B) obtained from CO desorption at 25 °C for 30 min (Fig. 3) are 0.91 for NiAl-C and 0.47 for NiAl-PC, respectively. Generally, the L/B ratio is increased with the decreasing Ni particle size [19–22], because CO preferentially linearly bonds to defect sites, whereas it is more favorable bridged bonds to close packed sites, and smaller particles generally contain higher concentration of defect sites than those of larger particles. However, the L/B ratio is not only depended on particle size, but also other factors, especially morphology. Blackmond and Ko reported two supported Ni catalysts with identical particle size shows different L/B ratio, as a result of different Ni particle morphology [19]. The particle

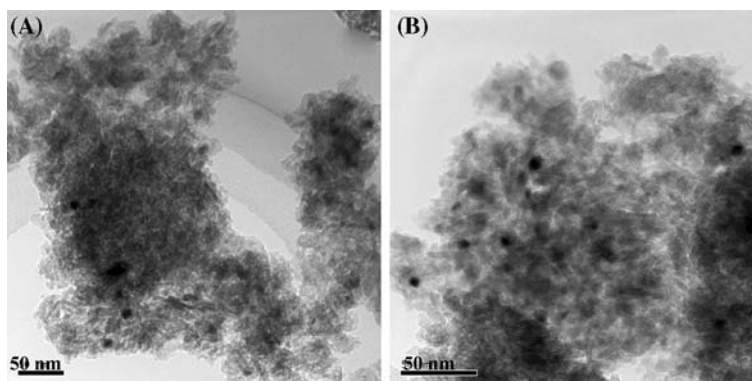
with smooth surface (low concentration of defect sites) gives smaller L/B ratio. The significantly decrease of L/B ratio of NiAl-PC with regard to that of NiAl-C cannot be related to particle size in the present study, as confirmed by TEM and XRD results. Figures 4 and 5 show the TEM images of fresh reduced catalysts and Ni particle size distributions, respectively. The TEM results show smaller Ni particle size for NiAl-PC ($d_n = 7.1$ nm) than that for NiAl-C ($d_n = 11.1$ nm). Figure 6 shows the XRD patterns of reduced catalysts. The Ni particle size calculated by Scherrer formula using the width at half maximum of Ni(200) peak, are 10.1 and 7.3 nm for the reduced NiAl-C and NiAl-PC, respectively, which is in good line with the TEM results. Therefore, we believe the significant decrease of the CO_L/CO_B ratio for NiAl-PC is related to morphology changes, indicating that NiAl-PC contains higher concentration of close packed plane (Ni particle surface is more smooth) than that of NiAl-C.

Temperature programmed desorption was performed to get the information of Ni-CO strength. All spectra were normalized to the spectrum with the largest integrated intensity, as shown in Fig. 7. For both catalysts, the relative intensity of the linear adsorbed CO band (CO_L) decreases linearly as temperature increases. Also for both catalysts, the relative intensity of bridge adsorbed CO band (CO_B) initially increases to maximum, and then decreases continuously. The initial increase of the CO_B can be attributed to linearly adsorbed CO being converted to bridge adsorbed CO, since bridge adsorbed CO is more stable. The relative total adsorbed CO intensity (CO_T = CO_L + CO_B) decreases continuously without the maximum. The relative CO_T intensity of NiAl-C decreases only slightly faster than that of NiAl-PC, which probably stems from the smaller portion of bridge adsorbed CO on the NiAl-C sample.

3.2 Activity and Coke Formation

The activity test was performed at 750 °C for 5 h, followed by an in situ TPO to evaluate coke formation. The activity

Fig. 4 TEM images of fresh hydrogen reduced (A) NiAl-C and (B) NiAl-PC



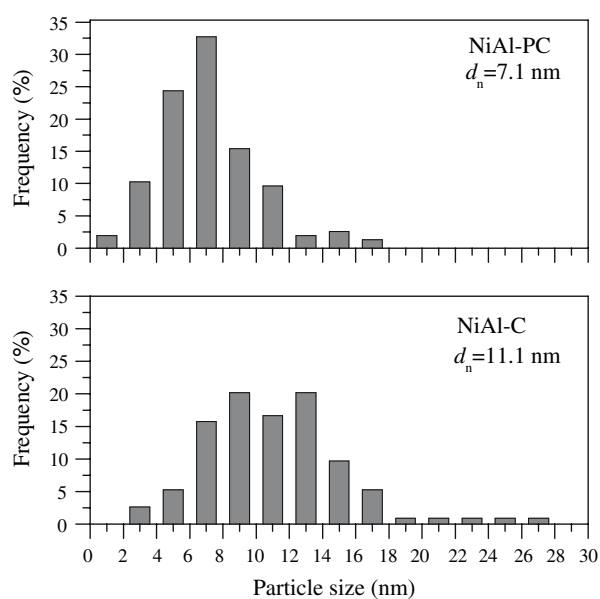


Fig. 5 Ni particle size distribution of fresh reduced NiAl-C and NiAl-PC obtained from TEM. Number-weighted particle size: $d_n = \sum n_i d_i / \sum n_i$ [4]

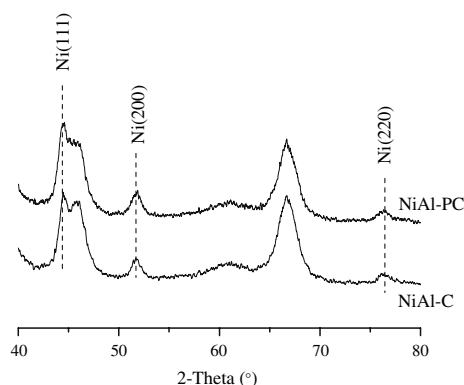


Fig. 6 XRD patterns of fresh reduced NiAl-C and NiAl-PC

results are summarized in Table 1 and the TPO results are shown in Fig. 8.

Both CH_4 and CO_2 conversions are about 6% higher over NiAl-PC than those over NiAl-C at the beginning of reaction (15 min). NiAl-PC maintained its activity at the end of 5 h run, and NiAl-C slightly decreased its activity. However, the specific CH_4 conversion rate, turnover frequency (TOF), which is defined as CH_4 conversion per surface Ni atom per second, is much higher for the NiAl-C sample. The lower TOF for NiAl-PC sample is believed as a result of higher concentration of close packed plane, since the methane activation is slower on these sites [5–7].

The TPO profile for the NiAl-C sample shows a small CO_2 peak at 96 °C and an intense peak at 636 °C, starting at 310 °C and ending at 817 °C, indicating it contains

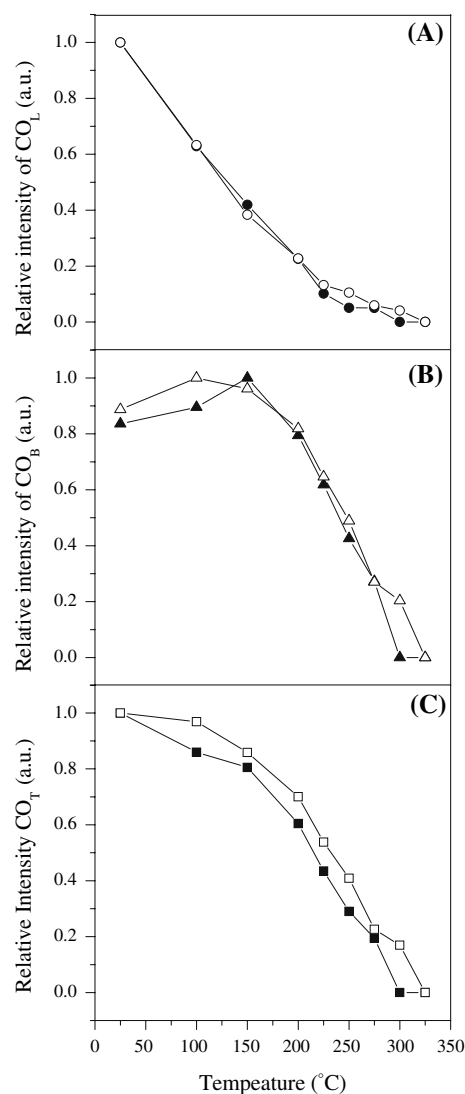


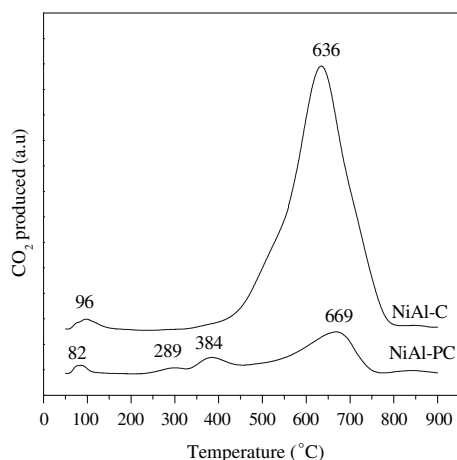
Fig. 7 Relative intensity of CO adsorbed on reduced NiAl-C (filled symbols) and NiAl-PC (open symbols) catalysts during temperature programmed desorption of CO. (A) linear adsorbed CO (CO_L); (B) bridge adsorbed CO (CO_B); (C) total adsorbed CO (CO_T)

different types of carbon species. For the NiAl-PC sample, three main peaks centered at 82 °C, 384 °C, and 669 °C as well as a very weak peak at 289 °C are present. It is generally accepted that several kinds of carbon existed in the Ni catalyst: very active monatomic carbon, filamentous carbon and encapsulating carbon, and amorphous and/or graphitic carbon deposited on the support [8, 28, 29]. Filamentous carbon has no effect on the activity of the catalyst, but a large amount of filamentous carbon destroy the catalyst particles and plug the reactor for a long-term run. Encapsulating carbon is responsible for the deactivation of the catalyst. The oxidation sequence for different types of carbon is dependent on the distance from the Ni particle, with the nearest carbon oxidized firstly by O_2 . Carbon

Table 1 Activities of NiAl-C and NiAl-PC at 15 min and 5 h time on stream at 750 °C

Sample	Activity at 15 min		Activity at 5 h		TOF ^a at 15 min (s ⁻¹)
	CH ₄ Con (%)	CO ₂ Con (%)	CH ₄ Con (%)	CO ₂ Con (%)	
NiAl-C	75	80	73	79	1.48
NiAl-PC	81	86	81	86	1.02

^a TOF, turnover frequency, defined as CH₄ conversion per surface Ni atom per second, Ni dispersion is estimated from $D\% = 100/d_{\text{TEM}}$ [31]

**Fig. 8** TPO profiles of NiAl-C and NiAl-PC after 5 h time on stream at 750 °C

species oxidized at temperatures lower than 100 °C can be assigned to reactive monatomic carbon, which is the intermediate of the reaction [4, 8, 30, 31]. For the NiAl-PC sample, the peaks at 289 °C and 384 °C can be attributed to Ni₃C, which is the closest to the Ni particle. The difference in oxidation temperature may be the result of different locations. Since the peak at 636 °C is very broad for NiAl-C, it can be assigned to a combined contribution from Ni₃C, filamentous carbon, encapsulating carbon, and carbon on the support. The TPO profile of the NiAl-C sample is very similar to the reported TPO profile of Ni/ γ -Al₂O₃ [32,33]. The peak at 669 °C in the NiAl-PC sample is probably generated from the amorphous carbon on the support. The integrated peak intensity for temperatures higher than 250 °C is about 5.1 times higher for the NiAl-C than for NiAl-PC. Moreover, the high temperature peak for NiAl-PC ends at 761 °C, which is 56 °C lower than NiAl-C. Combined with the results of TEM observations of catalysts after reaction [34] and TPO, it can be concluded that the formation of filamentous carbon and encapsulating carbon is greatly inhibited for the NiAl-PC sample. These results strongly support the superior anti-coke property of the plasma treated sample.

The lower methane TOF over close packed plane is expected gives rise to a lower amount of monatomic carbon than that over defect sites. The produced carbon can be

quickly removed by CO₂, leading to lower amount of coke formation. Therefore, a better balance between carbon formation due to methane decomposition and carbon gasification by CO₂ can be obtained. This expectation is confirmed by TPO results, which showed a significantly coke inhibition over NiAl-PC with respect to NiAl-C.

4 Conclusion

CO adsorbed IR study showed that the glow discharge plasma treated Ni/Al₂O₃ contains higher concentration of close packed plane. The specific CH₄ conversion rate (TOF) over close packed plane is slower than that over defect sites, leading to smaller amount of carbon produced. The carbon can be quickly removed by CO₂. Therefore, a better balance between carbon formation due to CH₄ decomposition and carbon gasification by CO₂ can be obtained over the plasma treated Ni/Al₂O₃ catalyst, resulting in a significant improvement of anti-coke property of the Ni catalysts.

Acknowledgment The supports from 973 project (under contract 2005CB221406) and National Natural Science Foundation of China (under contract 20490203) are greatly appreciated.

References

1. Takanabe K, Nagaoka K, Aika KI (2005) *Catal Lett* 102:153
2. Shamsi A (2006) *Catal Lett* 109:189
3. Wei JM, Iglesia E, (2004) *J Catal* 224:370
4. Bradford MCJ, Vannice MA (1996) *Appl Catal A* 142:97
5. Choudhary TV, Goodman DW (2000) *J Mol Catal A* 163:9
6. Burghgraef H, Jansen APJ, Santen RAV (1995) *Surf Sci* 324:345
7. Rostrup-Nielsen JR, Nørskov JK (2006) *Top Catal* 40:45
8. Trimm DL (1999) *CatalToday* 49:3
9. Rostrup-Nielsen JR, Hansen J-HB (1993) *J Catal* 144:38
10. Nikolla E, Holewinski A, Schwank J, Linic S (2006) *J Am Chem Soc* 128:11354
11. Juan-Juan J, Román-Martínez MC, Illán-Gómez MJ (2006) *Appl Catal A* 301:9
12. Zhu XL, Huo PP, Zhang YP, Liu CJ (2006) *Ind Eng Chem Res* 45:8604
13. Crisafulli C, Scirè S, Maggiore R, Minicò S, Galvagno S (1999) *Catal Lett* 59:21
14. Crisafulli C, Scirè S, Minicò S, Solarino L (2002) *Appl Catal A* 225:1
15. JAC Dias, Assaf JM (2004) *J Power Sources* 130:106

16. Blyholder G (1964) *J Phys Chem* 68:2772
17. Primet M, Dalmon JA, Martin GA (1977) *J Catal* 46:25
18. Rochester CH, Terrell RJ (1977) *J Chem Soc Faraday Trans I* 73:609
19. Blackmond DG, Ko EI (1985) *J Catal* 96:210
20. Wielers AFH, Aaftink GJM, Geus JW (1985) *Appl Surf Sci* 20:564
21. Peri JB (1984) *J Catal* 86:84
22. Anderson JA, Rodrigo MT, Daza L, Mendioroz S (1993) *Langmuir* 9:2485
23. Hadjiivanov K, Mihaylov M, Klissurski D, Stefanov P, Abadjieva N, Vassileva E, Mintchev L (1999) *J Catal* 185:314
24. Mihaylov M, Hadjiivanov K, Knözinger H (2001) *Catal Lett* 76:59
25. Derrouiche S, Bianchi D (2006) *Appl Catal A* 313:208
26. Shen WM, Dumesic JA, Hill CG (1981) *J Catal* 68:152
27. Rao KM, Spoto G, Zechina A (1989) *Langmuir* 5:319
28. Zhang ZL, Verykios XE (1994) *Catal Today* 21:589
29. Hou ZY, Yokota O, Tanaka T, Yashima T (2003) *Catal Lett* 89:121
30. Erdohelyi A, Cserenyi J, Solymosi F (1993) *J Catal* 141:287
31. Mark MF, Maier WF (1994) *Angew Chem Int Ed Engl* 33:1657
32. Wang SB, Lu GQM (1998) *Appl Catal B* 16:269
33. Wang SB, Lu GQ (1999) *Ind Eng Chem Res* 38:2615
34. Zhu XL, Zhang YP, Cheng DG, Liu CJ (2007) Structure and reactivity of plasma treated Ni/Al₂O₃ catalyst for CO₂ reforming of methane. Submitted, 2007